Engineering the Propeptide of Microbial Transglutaminase Zymogen: Enabling Substrate-Dependent Activation for Bioconjugation Applications

Ariyoshi, Ryutaro
Department of Applied Chemistry, Graduate School of Engineering, Kyushu University

Matsuzaki, Takashi
Department of Applied Chemistry, Graduate School of Engineering, Kyushu University

Sato, Ryo
Department of Applied Chemistry, Graduate School of Engineering, Kyushu University

Minamihata, Kosuke
Department of Applied Chemistry, Graduate School of Engineering, Kyushu University

他

出版情報：Bioconjugate Chemistry. 35 (3), pp.340-350, 2024-02-29. American Chemical Society (ACS)
バージョン：

Engineering the Propeptide of Microbial Transglutaminase Zymogen: Enabling Substrate-Dependent Activation for Bioconjugation Applications

*Ryutaro Ariyoshi[a], Takashi Matsuzaki[a], Ryo Sato[a], Kosuke Minamihata[a], Kounosuke Hayashi[a], Taisei Koga[a], Kensei Orita[a], Riko Nishioka[a], Rie Wakabayashi[a], Masahiro Goto[a,b], Noriho Kamiya[a,b]**

[a] Department of Applied Chemistry, Graduate School of Engineering, Kyushu University, 744 Motooka, Fukuoka 819-0395, Japan.

[b] Division of Biotechnology, Center for Future Chemistry, Kyushu University, 744 Motooka, Fukuoka 819-0395, Japan.

*Corresponding author. E-mail address: kamiya.noriho.367@m.kyushu-u.ac.jp

ABSTRACT

Microbial transglutaminase (MTG) from *Streptomyces mobaraensis* is a powerful biocatalytic glue for site-specific crosslinking of a range of biomolecules and synthetic molecules that have an MTG-reactive moiety. The preparation of active recombinant MTG requires post-translational proteolytic digestion of a propeptide that functions as an intramolecular chaperone to assist the correct folding of MTG zymogen (MTGz) in the biosynthesis. Herein, we report engineered active zymogen of MTG (EzMTG) that is expressed in soluble form in the host *Escherichia coli* cytosol and exhibits crosslinking activity without limited proteolysis of the propeptide. We found that saturation mutagenesis of residues K10 or Y12 in the propeptide domain generated several active MTGz mutants. In particular, the K10D/Y12G mutant exhibited catalytic activity comparable to that of mature MTG. However, the expression level was low possibly because of decreased chaperone activity and/or the promiscuous substrate specificity of MTG, which is potentially harmful to the host cells. The K10R/Y12A mutant exhibited specific substrate-dependent reactivity toward peptidyl substrates. Quantitative analysis of the binding affinity of the mutated propeptides to the active site of MTG suggested an inverse relationship between the binding affinity and the catalytic activity of EzMTG. Our proof-of-concept study provides insights into the design of a new biocatalyst using the MTGz as a scaffold, and a potential route to high-throughput screening of EzMTG mutants for bioconjugation applications.

KEYWORDS: Microbial transglutaminase, Propeptide, Protein labeling, Substrate specificity, Zymogen.

Introduction

Enzymes are natural proteinaceous catalysts that show diverse reaction specificity and thus are widely used from basic science to practical applications. Transglutaminase (TGase, protein-glutamine γ-glutamyltransferase, EC 2.3.2.13), widely found in microorganisms[4], plants[5], insects[6], and mammals[7,8], works as a natural glue by crosslinking the γ-carboxyamide groups of glutamine and a variety of primary amines, including the ε-amino group of lysine[4,9]. Microbial transglutaminase (MTG) from *Streptomyces mobaraensis* is a stable, Ca^{2+}-independent enzyme[10–12]. Because of its promiscuous specificity for proteinaceous substrates, MTG has rapidly been applied in the food industry as edible glue[12]. MTG has also been recognized as a powerful tool in bioconjugation applications, such as crosslinking of single-chain antibodies and enzymes[13], and bioconjugation of protein of interest with small chemical entities[14–17]. MTG can also recognize synthetic macromolecules such as polymers bearing MTG-reactive moieties[18–20] or chemically-modified nucleic acids[21]. Recently, MTG has been actively employed in the preparation of antibody-drug conjugates (ADCs) and bioimaging[22–24], suggesting further biological and biotechnological applications in biopharmaceutical industries.

However, the promiscuity of substrate recognition by MTG limits its utility as a biocatalytic glue, especially for *in vivo* applications that requires high substrate specificity [R2, R3]. MTG is expressed as an inactive zymogen, a precursor of the mature form, with a propeptide that functions as an intramolecular chaperone that assists correct folding[25–28] and shields the host cells from deleterious crosslinking of endogenous proteins by the MTG. The expression of active MTG is thus associated with proteolytic cleavage of the propeptide upon secretion[29,30]. Proteases from Streptomyces mobaraensis such as TGase-activating metalloprotease (TAMEP)[29] and tripeptidyl aminopeptidase (SM-TAP)[30] were identified to cleave the C-terminus of the propeptide with the recognition sites

of S↓FRAPDSD and FRAP↓DSD, respectively. In *Escherichia coli*-based expression systems, *in vitro*[31] or *in vivo*[32,33] post-translational treatment by a specific protease is required to obtain active recombinant MTG. Alternatively, co-expression of genes encoding the propeptide and mature MTG was found to yield the active form [R4, R5], though additional purification steps were needed to separate the two components.

To dissect the substrate specificity of MTG, researchers explored highly reactive peptidyl substrates by using a phage display system[34] and designed a pair of engineered small proteinaceous substrates and MTG mutants by protein engineering.[35] Although the combination of rational design and screening is an important option for further engineering of MTG, direct expression of the gene encoding mature MTG in the cytosol of host cells such as *E. coli*[33] is difficult, which hampers the construction of mutant libraries to tune its substrate specificity.[36] To overcome this limitation, a protease-mediated self-cleavable system[R6 (Ref.49)] and an intein-mediated self-splicing system[R7] were designed for intracellular production of active MTG from its zymogen in *E. coli* and *Corynebacterium glutamicum*, respectively. High-throughput screening (HTS) of active MTG by post-translational proteolysis of zymogen mutants displayed on the yeast surface was investigated,[37] but it is still difficult to validate the substrate specificity of soluble MTG mutants by HTS. ~~In this context, other "glue enzymes" with narrower substrate specificities in comparison with MTG such as sortase A, have increased utility for researchers.[38]~~ Searching other organisms producing TGases that are potentially applicable to highly specific bioconjugation is also an important option and KalbTG isolated from *Kutzneria albida* was reported to be more compatible with the preparation of ADCs than MTG.[39]

The control of enzymatic activity is vital for the spatio-temporal control of both activation and inhibition to sustain the cellular physiology in the host organisms. For example, proteases are often

present as a zymogen to control the proteolytic digestion of proteinaceous endogenous constituents in the host organisms.[1,2] Interestingly, zymogens can show weak reactivity toward specific substrates[3], implying that modulation of the interaction of the propeptide with the enzyme active site may increase the frequency of substrate entry into the active site. In fact, the enzymatic activity of some proteases was markedly enhanced by the deletion of several amino acids adjacent to propeptide[3]. Accumulated knowledge about natural and artificial strategies to modulate the activity of zymogens motivated us to engineer the scaffold of zymogen as a base structure for the design of a new biocatalyst.

Herein, we propose novel engineered active zymogen of MTG (EzMTG) (**Figure 1**). Our concept to create active, soluble recombinant MTGs that can be expressed in the *E. coli* cytosol is to simply substitute two amino acids in the propeptide ~~(residues K10 and Y12)~~ to suppress the self-crosslinking (K10) and relieve the interaction with the active site of MTG[40] (Y12) to allow substrate entry while keeping the intramolecular chaperone functionality of the propeptide. Saturation mutagenesis of each amino acid led to the K10D/Y12G mutant, which exhibits crosslinking activity comparable to that of the mature counterpart. We also found that the K10R/Y12A mutant exhibits higher reactivity toward peptidyl substrates than small molecular substrates, by which the possibility of substrate-dependent switch-on crosslinking activity was shown. Our results open a way to generate new MTG mutants with altered substrate specificity, and illustrate the potential of engineering the scaffold of naturally occurring enzyme precursors toward new enzymatic functions.

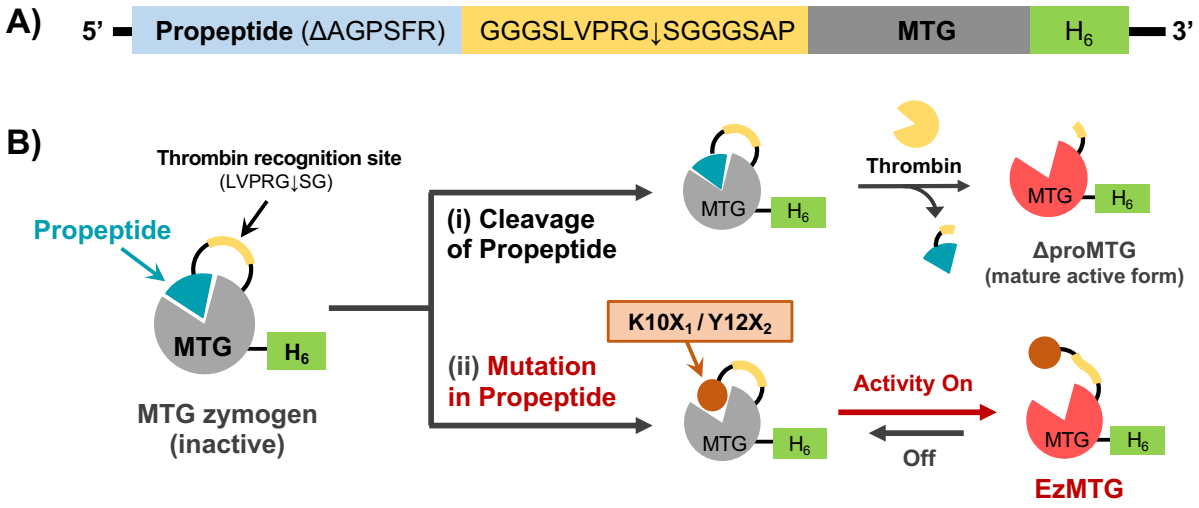

100

101 **Figure 1** EzMTG constructs evaluated in this study. (A) Schematic illustration of DNA constructs
102 encoding EzMTG. (B) Schematic illustration of the preparation of recombinant active mutants
103 from MTG zymogen (MTGz) (i) by proteolytic cleavage using thrombin, and (ii) by designing a
104 mutated propeptide to modulate the interaction with the active site.

105

106 **Results and discussion**

107

108 **Design of EzMTG based on the zymogen scaffold**

109 To validate our concept (shown in **Figure 1)**, a series of mutants of recombinant MTG zymogen
110 was designed (**Figure S1**). First, we designed the base protein scaffold of EzMTG by replacing
111 part of the C-terminal sequence (AGPSFR) of the propeptide domain with a thrombin cleavage site
112 surrounded by a Gly-Ser flexible linker (GGGS LVPRGS GGGS). The insertion of the flexible
113 linker is expected to facilitate proteolysis by thrombin to produce recombinant mature MTG with
114 a C-terminal His_6-tag (ΔproMTG). We selected the C-terminus of the propeptide for the insertion
115 of the protease cleavage site by referring the maturation process of native MTG. Previously, pro-
116 tease from *Streptomyces mobaraensis* such as TGase-activating metalloprotease (TAMEP) was
117 identified to cleave the C-terminus of the propeptide in the host cell[29]. Dispase was also used to

cleave the propeptide in the production of active recombinant MTG[31]. In addition, we selected LVPRG↓SG sequence to avoid the generation of α-amino group at the N-terminal Gly after the cleavage, which can be a reactive site for MTG-catalyzed crosslinking[R1]. ΔproMTG was used as the positive control in this study. Next, by referring to the results of crystal structure analysis of the MTG precursor, which showed that residue Y12 in the propeptide is crucial for strong binding between the propeptide and the active site of the mature form,[40] we selected Y12 as the starting point to engineer the scaffold of the zymogen. Unexpectedly, we found that point mutation of Y12 to Ala (Y12A) made MTG self-reactive as this mutant was self-labeled with an MTG-reactive fluorescent peptidyl substrate, FITC-β-Ala-QG (**Figure S2**). These results indicate that the single mutation Y12A could promote the activation of the MTG zymogen. Further studies showed that the replacement of K10 totally suppressed the self-labeling (**Figure S3**). The replacement of K10 is useful to suppress the self-labeling of MTG with a small molecule that could reduce the active fraction of the catalyst in the reaction mixture and the self-crosslinking with a substrate protein that would increase the heterogeneity of reaction products. On the basis of these serendipitous findings, residues K10 and Y12, located in the propeptide domain, were selected as the mutation sites to design EzMTGs.

Expression and enzymatic activity of K10X/Y12A mutants

We first prepared the series of K10X/Y12A mutants by saturation mutagenesis of K10 to the other 19 natural amino acids normally found in proteins. The initial screening of catalytic activity was done by a standard hydroxamate assay using benzyloxycarbonyl-L-glutaminylglycine (Z-QG) and hydroxylamine (**Figure S4 (i)**). **Figure 2** showed that replacement of K10 with D or E increased the catalytic activity, although much smaller than that of mature MTG (ca. 23 U/mg[49]).

The results imply the presence of electrostatic repulsion around the K10 position on the protein surface, thereby facilitating the recognition of small substrates. The K10G/Y12A mutant showed comparable activity to that of K10E/Y12A mutant. By contrast, the low catalytic activity of the K10R/Y12A and K10H/Y12A mutants suggests that mutated propeptide remained the native-like structure if K10 was substituted by a basic amino acid. The other 14 mutants showed low catalytic activities.

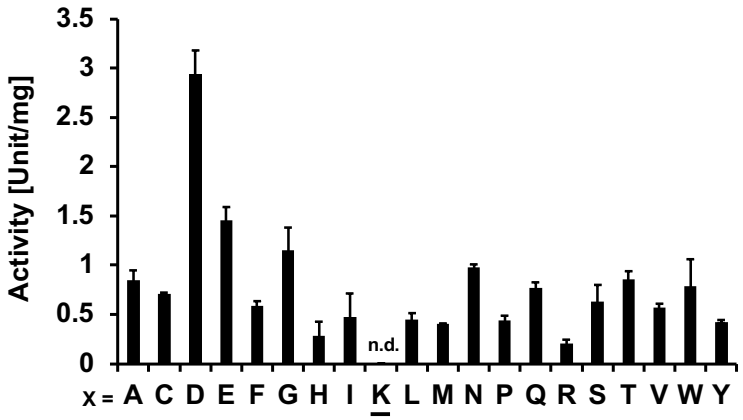

Figure 2 Enzymatic activity assay of K10X/Y12A MTGz mutants by hydroxamate assay. Where X = K, the protein was the Y12A single mutant (n.d.: Not detected, below the detection limit). Data are presented as the mean ± standard deviation of three experiments (n = 3).

In terms of the protein expression, all mutants were found in the soluble fraction although each mutant showed a different yield, implying variation of the chaperone functionality of the mutated propeptides (**Figure S5(i)**). Notably, K10X/Y12A (X = D, E, G) mutants showed lower protein yields but higher catalytic activities than the other mutants. This trade-off relationship between the expression level of the soluble protein and its catalytic activity is likely due to cytotoxicity caused by the lack of activity regulation of MTG mutants in the *E. coli* cytoplasm (**Figure S6**). The yield

of the Y12A single mutant decreased possibly due to self-crosslinking and/or intermolecular cross-linking with endogenous proteins in the purification steps.

Expression and enzymatic activity of K10R/Y12X mutants

We next focused on residue Y12 combined with K10R mutation where K10 was replaced with Arg to minimize the effect of the substitution by keeping a positive charge. In addition, since the K10R mutation sufficiently suppressed crosslinking activity whereas it showed sufficient protein expression in E. coli, the generation of K10R/Y12X double mutant library would be the most suitable for the evaluation of the second-round mutation at Y12 position. A series of double mutants (K10R/Y12X, X = 19 natural amino acids) was expressed in *E. coli* and the enzymatic activity of the purified enzymes was measured by a continuous GLDH-coupled assay (**Figure S4 (ii)**).[41] After the addition of MTG (0.15 μM) to the substrate solution containing cadaverine (primary amine substrate, 10 mM) and Z-QG (Gln-donor substrate, 20 mM), the catalytic activity was evaluated by the initial rates. The K10R/Y12G mutant exhibited the highest activity (**Figure 3**). Since Y12 constitutes part of the α-helical structure of the propeptide, substitution with Gly decreased the stability of the α-helix and may increase the accessibility of the active site by the substrate. The Y12D mutation also resulted in higher catalytic activity than the other mutants. Both of these mutants (K10R/Y12G and K10R/Y12D) showed low protein yields (**Figure S5(ii)**), so the activity/yield trade-off relationship was observed as for the K10X/Y12A mutants. The low yield of the K10R/Y12P mutant indicated that the substitution of Y12 by Pro, which is classified as an α-helix breaking amino acid due to the lack of forming hydrogen bonds inside α-helices[R8], significantly reduced the intramolecular chaperone functionality of the propeptide domain.

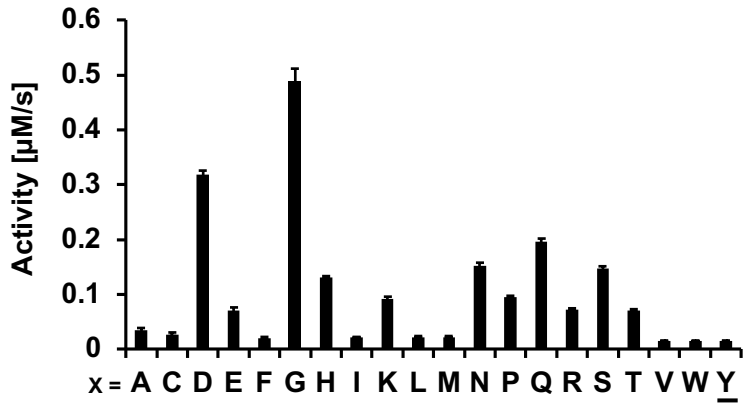

Figure 3 Enzymatic activity assay of K10R/Y12X mutants assessed by a continuous glutamine dehydrogenase -coupled assay for MTG activity. Where X = Y, the protein was the K10R single mutant. Data are presented as the mean ± standard deviation of three experiments (n = 3).

Characterization of K10X$_1$/Y12X$_2$ double mutants

Encouraged by the results for the K10X/Y12A and K10R/Y12X series of MTGz mutants, we investigated combined mutation at positions K10 and Y12 with R/D replacing K10 and A/G replacing Y12, respectively. We first compared the susceptibility of two mutants, K10R (single mutation) and K10R/Y12A, to thrombin digestion. SDS-PAGE analysis of the purified mutants before and after thrombin treatment suggested that the propeptide was cleaved off from the zymogen scaffold after substitution at Y12. By contrast, the K10R single mutant was found to be resistant to thrombin treatment (**Figure 4A**). The K10R mutant was not fully activated by thrombin digestion, whereas the specific activity of the K10R/Y12A mutant was the same as that of ΔproMTG after thrombin digestion (**Figure 4B**). These results suggest that the importance of the Y12 position for the susceptibility of the linker containing the thrombin-cleavage site to thrombin, which would also reflect the conformational flexibility around the propeptide.

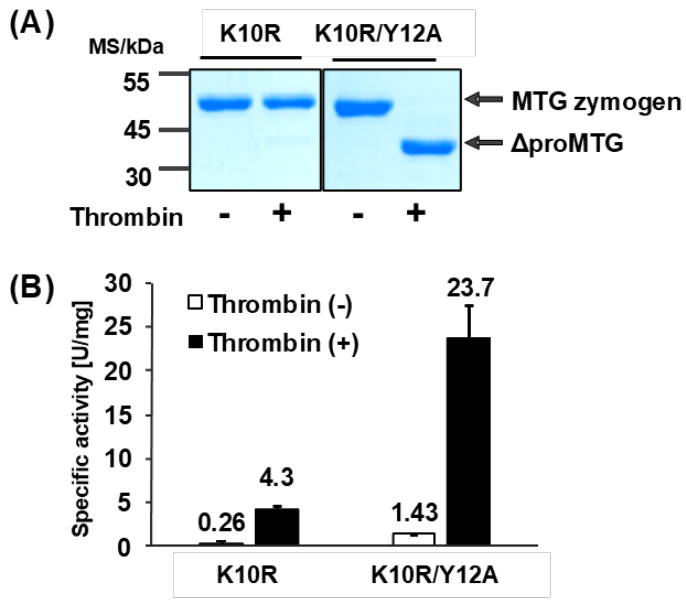

Figure 4 (A) SDS-PAGE analysis of purified K10R and K10R/Y12A MTGz mutants. (B) Specific activity of the mutants assessed by hydroxamate assay before and after thrombin digestion. Data are presented as the mean ± standard deviation of three experiments (n = 3).

Next, we conducted detailed kinetic analyses of four different types of EzMTG. From inspection of the relationship between the initial reaction rates and the substrate concentration, specificity constants (k_{cat}/K_m) were determined from the initial slope and were shown in **Figure 5A**. Y12G mutation had more impact on the increase in crosslinking activity than Y12A mutation for both of the K10R and K10D double mutants. The difference was markedly enhanced by the integration of mutation at K10 position, and interestingly the K10D/Y12G mutant exhibited a comparable specificity constant to that of ΔproMTG.

For further analysis of the substrate recognition by MTGz mutants, two mutants (K10D/Y12A and K10D/Y12G) were selected and kinetic parameters for the Gln-donor substrate (Z-QG) were determined (**Figure 5B**). The value of the specificity constant of the K10D/Y12G mutant was ca. 85% that of ΔproMTG and the K_m values were comparable even in the presence of propeptide in

the protein scaffold. By contrast, the K10D/Y12A mutant showed a ca. 80% decrease in the specificity constant compared with that of ΔproMTG, mainly owing to a ca. five-fold increase in the K_m value. These results suggest that the K10D/Y12A mutant is more susceptible to steric hindrance of substrate binding by the propeptide than the K10D/Y12G mutant.

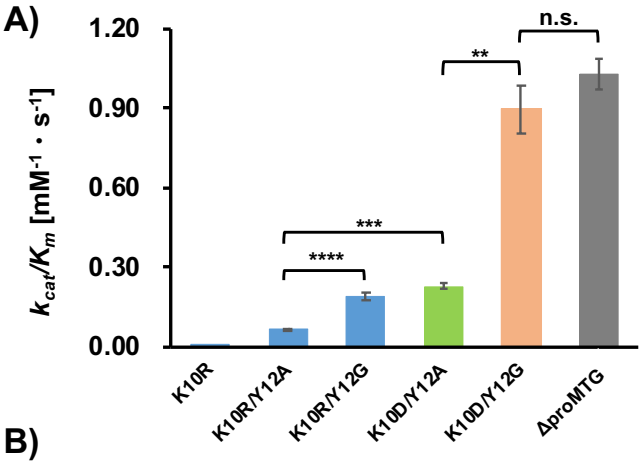

B)

enzyme	k_{cat} [s^{-1}]	K_m [mM]	k_{cat}/K_m [mM^{-1}s^{-1}]
K10D/Y12A	4.84 ± 0.33	21.4 ± 2.1	0.23 ± 0.01
K10D/Y12G	4.35 ± 0.09	4.90 ± 0.37	0.89 ± 0.07
ΔproMTG	4.85 ± 0.19	4.75 ± 0.38	1.05 ± 0.05

Figure 5 (A) Specificity constants (k_{cat}/K_m) of EzMTGs and ΔproMTG. (B) Kinetic parameters determined by using 2.5—30 mM Z-QG, 10 mM cadaverine and 0.15 μM enzyme in 0.2 M MOPS-EDTA buffer (pH 7.2). Data are presented as the mean ± standard deviation of three experiments ($n = 3$), $^{**}p < 0.01$, $^{***}p < 0.005$, $^{****}p < 0.001$, n. s. = not significant.

The stability of enzymes is a crucial factor for their practical application. Several point mutations have been reported to increase the thermal stability of mature MTG were reported.[42,43] We found that a significant decrease in the catalytic activity of the K10D/Y12G mutant upon thermal treatment (**Figure S7**). By contrast, the K10R and K10R/Y12A mutants showed comparable thermal

stability to that of ΔproMTG. These results imply the potential of MTGz mutants showing low activity as a target scaffold for protein engineering of EzMTG.

Binding affinity of mutated propeptide to the enzyme active site

To gain further insight into the effects of the mutated propeptides on substrate recognition by EzMTG, we designed fusion proteins composed of EGFP and mutated propeptide, EGFP-Pro($K10X_1/Y12X_2$), and they were subjected to bio-layer interferometry (BLI) analysis (**Figure. S7**).[44,45] To eliminate non-specific binding to the Ni-NTA-modified surface for BLI, ΔproMTG lacking the C-terminal His-tag (**Figure S1**) was prepared and used as the analyte (**Figure 6A**).

On the basis of the foregoing observations, K10R, K10R/Y12A and K10D/Y12G mutants, which showed different catalytic performance (**Figure 5A**) were selected for the analysis. As expected, EGFP-Pro(K10R) showed high affinity (dissociation constant; K_d = 19.0 nM) for ΔproMTG (**Figures 6B** and **6E**), which explains the low catalytic activity of the K10R mutant. Interestingly, the additional mutation of Y12 to Ala resulted in a ca. 410-fold reduction in the affinity (K_d = 7.85 μM) (**Figures 6C** and **6E**). This result indicates that the marked reduction of the binding affinity of mutated propeptide to the enzyme active site, leading to the generation of crosslinking activity towards small molecular substrates (Z-QG and cadaverine). Furthermore, quantitative analysis of EGFP-Pro(K10D/Y12G) was impossible (**Figure 6D**), indicating disruption of the tertiary structure of the propeptide, accounting for the comparable catalytic activity of the K10D/Y12G mutant to that of ΔproMTG and the low protein yield. These results demonstrate again that we must take both chaperone functionality and active site-binding affinity of the mutated propeptide into account in the design of EzMTGs.

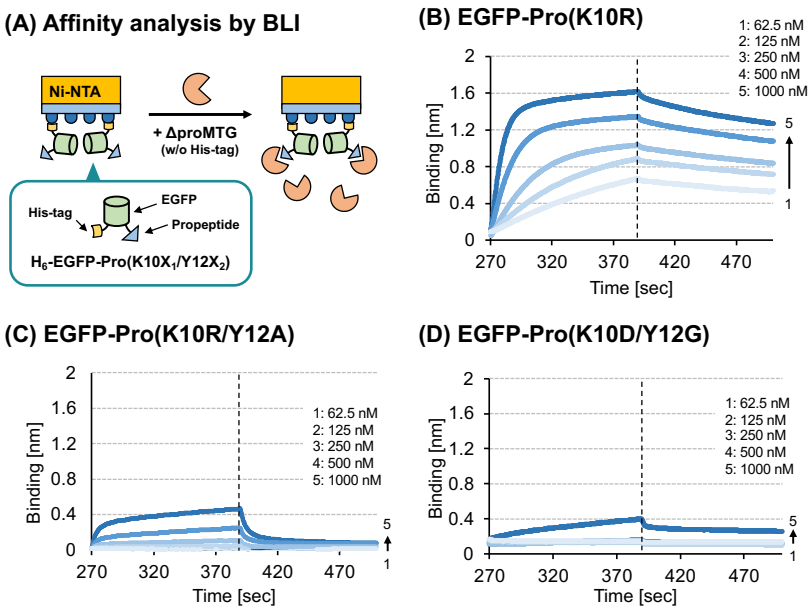

(E)

Mutated propeptide	k_a [M^{-1} s^{-1}]	k_d [s^{-1}]	K_D [M]
Pro(K10R)	1.13E05	2.16E-03	1.90E-08
Pro(K10R/Y12A)	9.00E03	7.07E-02	7.85E-06

Figure 6 Evaluation of binding affinity of mutated propeptide to the active site of MTG by bio-layer interferometry (BLI) analysis. (A) Schematic illustration of BLI analysis. (B)-(D) Association and dissociation profiles of ΔproMTG without His-tag to EGFP-Pro(K10R), EGFP-Pro(K10R/Y12A) or EGFP-Pro(K10D/Y12G) immobilized on the detection surface via Ni-NTA interaction. (E) Rate constants for association (k_a) and dissociation (k_d) and dissociation constants (K_D) determined from the profiles in (B) and (C).

Blood coagulation Factor XIII and TG2 are representative examples of mammalian TGases in which the catalytic activity is controlled by endogenous Ca^{2+} ions. Mammalian TGase consists of several domains that undergo large conformational changes upon activation.[46,47,48] Our results with EzMTG demonstrated that introduction of key mutations in propeptide domain could relieve the strong binding of the propeptide to the enzyme active site, enhancing the entry of substrates, thereby generating crosslinking activity of the MTG zymogen.

Application of EzMTG in site-specific protein labeling

Finally, we explored the potential of EzMTGs in protein labeling applications (**Figure S4 (iii)**). **Figure 7** shows SDS-PAGE analysis of the cross-linking reaction between tumor necrosis factor-alpha (TNF-α) fused with the N-terminal MRHKGS sequence (Ktag-TNF-α) and FITC-β-Ala-QG catalyzed by various forms of MTG. Fluorescence imaging showed that Ktag-TNF-α was successfully labeled with the fluorescent probe by ΔproMTG and all the EzMTGs except for the K10R mutant. Time-dependent increases in the fluorescence signal revealed that the trend of the cross-linking reaction was consistent with the order of catalytic activity shown in **Figure 5**. Notably, the K10R/Y12A mutant showed > 50% yield after incubation for 1 h, though this mutant exhibited ca. $1/10^{th}$ of the crosslinking activity of toward small molecular substrates (**Figure 5A**). These results indicate that the substrate recognition of EzMTG depends on the type of substrate and the affinity of the substrate for the active site of MTG (**Table 1**). This also suggests that the substrate preference can be further tuned by designing an HTS system with EzMTGs. Since the promiscuity of substrate recognition by MTG limits its utility for applications that necessitate homogeneous reaction products, it should be interesting to apply EzMTGs to construct an HTS of reactive peptide pairs in the *E. coli* cytosol[R9] because soluble expression of active mutants is possible. Further manipulation of EzMTGs would also extend extending our concept to other precursor enzymes.

Table 1 Characteristics of selected EzMTG mutants in this study.

Mutation	Activity [a] (for small substrates)	Activity [b] (for large substrates)	Expression in *E. coli* [c] (cell wet weight)
K10R	Low	Low	High
K10R/Y12A	Low	Moderate	Moderate

K10R/Y12G	Moderate	Moderate	Low
K10D/Y12A	Moderate	High	Low to moderate
K10D/Y12G	High	High	Low

[a] Based on the GLDH assay (**Fig. 5A**); [b] Based on the protein labeling assay (**Fig. 7**); [c] **Fig. S6**.

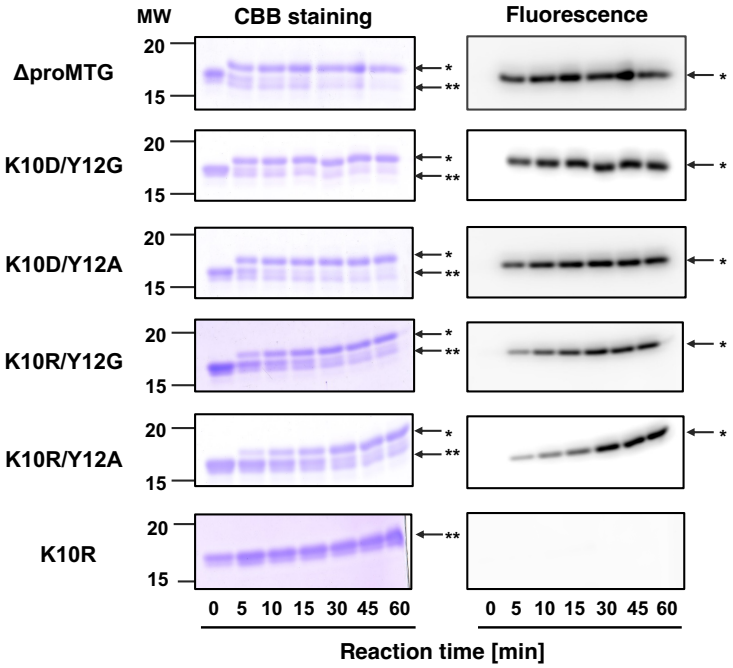

Figure 7 SDS-PAGE analysis of ΔproMTG- or EzMTG-mediated labeling of Ktag-TNFα with FITC-β-Ala-QG. The results of Coomassie Brilliant Blue staining (left) and the fluorescence (right) of the gel. *FITC-labeled Ktag-TNFα, **Non-labeled Ktag-TNFα.

Conclusion

Our concept of EzMTG is a straightforward way to promote the activation of MTG zymogen without limited proteolysis by either inducing conformational fluctuation in the propeptide domain or keeping the chaperone functionality. Our proof-of-concept study will lead to generation of comparable catalytic performance to that of mature MTG but with altered substrate specificity, as

exemplified by the K10R/Y12A mutant that exhibited improved crosslinking activity toward peptidyl substrates. Tuning of the substrate preference by modulating the intramolecular inhibitory domain of an enzyme provides insight for the design of a new biocatalyst from these precursors. Since EzMTGs can be expressed in soluble form in the *E. coli* cytosol, our results provide an opportunity for HTS of active MTG zymogen mutants for *in vivo* bioconjugation applications.

Materials and methods

1. Materials

PrimeSTAR® MAX DNA Polymerase and an In-Fusion® HD Cloning Kit were purchased from Takara Bio Inc. (Shiga, Japan). LB broth (Miller) was purchased from Merck Millipore Corp (Billerica, MA, USA). Tryptone, dried yeast extract, tris(hydroxymethyl)aminomethane (Tris) and a Rapid Stain CBB Kit were purchased from Nacalai Tesque, Inc. (Kyoto, Japan). Hydrochloric acid, sodium chloride, potassium chloride, disodium hydrogen phosphate 12-H_2O, dipotassium hydrogen phosphate, and potassium dihydrogen phosphate were purchased from Fujifilm Wako Pure Chemical Corporation (Osaka, Japan). Benzyloxycarbonyl-L-glutaminylglycine (Z-QG), α-ketoglutarate, glutamine dehydrogenase (GLDH) and cadaverine were purchased from Sigma Aldrich (St. Louis, USA). β-NADH were purchased from Oriental Yeast Inc. (Shiga, Japan). Gradient gels (5-20%) for SDS-PAGE was purchased from Atto Corporation (Tokyo, Japan). N-Ethylmaleimide was purchased from Kishida Chemical Co., Ltd. (Osaka, Japan). Ultrapure water supplied by a Milli-Q® Reference Water Purification System (Merck Millipore Corp.) was used for buffer preparation. MTG was recombinantly prepared by *Escherichia coli* BL21 star (DE3) as previously reported[49].

2. Construction of MTG zymogen (MTGz) mutants

The pET22b+ vector carrying the gene encoding K10R/Y12A MTGz[49] was used as the template DNA for vector construction of K10X/Y12A and K10R/Y12X mutants (X = 20 natural amino acids). To construct the vector containing the MTGz mutants, some mutations were introduced by inverse PCR and self-ligation of the PCR products, introducing a DNA sequence encoding a thrombin cleavage sequence (LVPRGS) between the propeptide and mature MTG. The amino acid sequences and schematic illustrating of all the MTGz mutants used in this study are summarized in **Table S1**.

3. Expression and purification of recombinant proteins

3.1 K10X/Y12A and K10R/Y12X MTGz mutants

The expression of the MTGz mutants was conducted with *E. coli* BL21 star (DE3). The plasmid vectors encoding MTG mutants were transformed into the cells by heat shock and cultured on a lysogeny broth plate containing 100 μg/mL sodium ampicillin. A single colony was inoculated into 3.5 mL of lysogeny broth containing the same amount of sodium ampicillin and shaken at 220 rpm at 37 ˚C for 4 h. Preculture of cells expressing K10X/Y12A MTGz were placed into 25 mL of Terrific broth medium containing 100 μg/mL ampicillin and cultured with shaking at 220 rpm at 37 ˚C until $OD_{600\ nm}$ reached 0.5. The expression of K10X/Y12A MTGz mutants was induced by the addition of 1 mM isopropyl-β-D-thiogalactoside (IPTG) and followed by shaking at 18 ˚C. K10R/Y12X MTGz mutants were cultured with Auto Induction Medium. The cells were harvested by centrifugation at 5,000 × g for 20 min and the supernatant was discarded. The pellet was resuspended in phosphate-buffered saline (PBS, pH 7.4) and frozen at −80 ˚C until protein purification.

For the purification of MTGz mutants, the cell pellet was thawed in running water. The cell suspension was sonicated on ice for 3 min. The cell debris was removed by centrifugation at 16,000 × g for 10 min at 4 ˚C. The supernatants were initially applied to a HisGraviTrap column (GE Healthcare Life Sciences, Chicago, IL, USA), which was pre-equilibrated with HisTrap binding buffer (20 mM Tris-HCl, 500 mM NaCl, 35 mM imidazole, pH 7.4). The columns were washed with the same buffer until all the unbound proteinaceous substances were eluted, and then the peptide tag fused proteins were eluted with a HisTrap elution buffer (20 mM Tris-HCl, 500 mM NaCl, 500 mM imidazole, pH 7.4). The fractions containing MTGz were concentrated, and the buffer was exchanged to binding buffer (1×PBS with 0.1 mM dithiothreitol, pH 7.4) by membrane filtration using 10 kDa MWCO Amicon Ultra-15 Centrifugal Filter Units (Billerica, MA, USA). The purified MTGz were concentrated using the ultrafiltration membrane that was suitable for each protein. Final protein concentrations of MTG mutants were quantified using YabGelImage software (https://sites.google.com/site/yabgel/home) using bovine serum albumin (BSA) as a standard protein.

3.2 MTGz mutants selected for kinetic analysis

The expression of K10R, K10R/Y12A, K10R/Y12G, K10D/Y12A, K10D/Y12G MTGz were conducted with *E. coli* BL21 star (DE3). The plasmid vector encoding the MTGz mutant was transformed into the cells by a heat shock method and transformants were cultured on lysogeny broth plates containing 100 μg/mL sodium ampicillin. A single colony was inoculated into 3.5 mL of lysogeny broth containing the same amount of ampicillin sodium and shaken at 220 rpm at 37 ˚C for 6 h. This preculture medium was transferred into 1 L of Terrific Both medium containing the same antibiotics and cultured with shaking at 220 rpm at 37 ˚C until OD_{600} reached around 0.5. Protein expression was induced by addition of IPTG to a final concentration of 0.1 mM, and the

cells were cultured overnight at 18 ˚C. The cells were harvested by centrifugation at 5,000 × g for 20 min and the supernatant was discarded. The pellet was resuspended in PBS (pH 7.4) and frozen at −80 ˚C until protein purification. To follow the cell growth, samples were withdrawn from the cell culture medium every few hours and the OD_{600} was measured. The wet weight of cells was calculated by subtracting the weight of an empty bottle from that of the harvested cell pellet.

For the protein purification, the pellet was thawed with running water. The cell suspension was sonicated on ice for 12.5 min. The cell debris was removed by centrifugation at 15,000 × g for 10 min at 4 ˚C. The supernatants were initially applied to a HisTrap FF crude 5 mL column (GE Healthcare UK Ltd.), which was pre-equilibrated with HisTrap binding buffer (20 mM Tris-HCl, 500 mM NaCl, 35 mM imidazole, pH 7.4). The column was washed with the same buffer until all of the unbound proteinaceous substances eluted, and MTG mutant was eluted by a gradient of HisTrap elution buffer (20 mM Tris-HCl, 500 mM NaCl, 500 mM imidazole, pH 7.4) up to 100% over 13 column volumes. The fractions containing the MTG mutant was concentrated, and the buffer was exchanged to HiTrap binding buffer (10 mM Tris-HCl, pH 8.0) by membrane filtration of 10 kDa MWCO Amicon Ultra-15 Centrifugal Filter Units. The desalted solution containing protein of interest was applied to a HiTrap Q HP 5 mL column (GE Healthcare UK Ltd.) pre-equilibrated with HiTrap binding buffer. The column was washed with five column volumes of the same buffer, and peptide tag fused proteins were eluted by a gradient of elution buffer (10 mM Tris-HCl, 500 mM NaCl, pH 8.0) up to 100% over 13 column volumes. The fractions containing peptide tag fused proteins were concentrated to approximately 5 mL using ultrafiltration membrane, and MTGz was then further purified with size exclusion chromatography using ProteoSEC-D 16/60 6-600 HR column (Protein Ark) with PBS (pH 7.4) including 0.1 mM dithiothreitol as the running buffer. The purified protein was concentrated using a suitable ultrafiltration membrane.

Protein concentration was determined by measuring the UV absorbance at 280 nm using NanoDrop. The extinction coefficient predicted by ExPASy ProtParam (https://web.expasy.org/protparam/) was used for calculation.

3.3 EGFP-Propeptide fusion proteins

The expression of the EGFP-Propeptide fusion proteins (EGFP-Pro($K10X_1/Y12X_2$), X_1 = R or D, X_2 = A or G) were conducted with *E. coli* BL21 star (DE3). The plasmid vectors encoding EGFP-Propeptide mutants were transformed into the cells by heat shock and cultured on a lysogeny broth plate containing 100 μg/mL sodium ampicillin. A single colony was inoculated into 3.5 mL of lysogeny broth containing the same amount of sodium ampicillin and shaken at 220 rpm at 37 ˚C for 4 h. The precultured medium of EGFP-Propeptide were placed into 25 mL of Terrific broth medium containing 100 μg/mL ampicillin and cultured with shaking at 220 rpm at 37 ˚C until $OD_{600\ nm}$ reached around 0.5. The expression of them were induced by the addition of 1 mM IPTG and followed by shaking at 18 ˚C. The cells were harvested by centrifugation at 5,000 × g for 20 min and the supernatant was discarded. The pellet was resuspended in PBS (pH 7.4) and frozen at −80˚C until protein purification.

For the purification of EGFP-Propeptide mutants, the pellet was thawed in running water. The cell suspension was sonicated on ice for 3 min. The cell debris was removed by centrifugation at 15,000 × g for 10 min at 4 ˚C. The supernatants were initially applied to a HisGraviTrap column (GE Healthcare Life Sciences, Chicago, IL, USA), which was pre-equilibrated with HisTrap binding buffer (20 mM Tris-HCl, 500 mM NaCl, 35 mM imidazole, pH 7.4). The column was washed with the same buffer until all the unbound proteinaceous substances were eluted, and then the peptide tag fused proteins were eluted with HisTrap elution buffer (20 mM Tris-HCl, 500 mM NaCl, 500 mM imidazole, pH 7.4). Fractions containing EGFP-Propeptide mutant were concentrated, and

the buffer was exchanged to HiTrap binding buffer (10 mM Tris-HCl, pH 8.0) by membrane filtration of 10 kDa MWCO Amicon Ultra-15 Centrifugal Filter Units. The desalted solution containing the protein of interest was applied to a HiTrap Q HP 5 mL column pre-equilibrated with the HiTrap binding buffer. The column was washed with five column volumes of the same buffer, and peptide tag fused proteins were eluted by a gradient of elution buffer (10 mM Tris-HCl, 500 mM NaCl, pH 8.0) up to 100% over 13 column volumes. The fractions containing an EGFP-Propeptide mutants was concentrated, and the buffer was exchanged to PBS (pH 7.4) by membrane filtration (10 kDa MWCO). Protein concentration was determined by measuring the UV absorbance at 280 nm using NanoDrop with the theoretical extinction coefficient of each protein.

3.4 K-tagged TNF-α

The synthetic gene encoding matured human TNF-α with an N-terminal K-tag sequence (MRHKGS) synthesized by and purchased from IDT Technologies was amplified by PCR and cloned into the pCold 4 vector using In-Fusion Cloning to construct the expression vector for K-tagged TNF-α (Ktag-TNFα). The vector was transformed into competent cells of *E. coli* BL21 star (DE3) using the heat shock method (42 ˚C for 30 sec) and cultured on an LB agar plate containing 100 μg/mL of ampicillin sodium. After incubating overnight at 37 ˚C, a single colony was picked and inoculated into 5 mL of LB medium containing the same amount of antibiotics and cultured overnight at 37 ˚C with shaking at 180 rpm. The precultured cell suspension was then transferred into 1 L of LB medium containing 100 μg/mL ampicillin sodium and cultured at 37 ˚C with shaking at 180 rpm until the OD_{600} reached 0.5. The cultured cell suspension was then cooled on ice for approximately 10 minutes to reduce the temperature to below 17 ˚C. Then, IPTG was added at a final concentration of 0.1 mM and the culture was continued for 12 h at 17 ˚C. The cells were collected by centrifugation at 5,000 × g for 20 min. The cells were washed with PBS(-) twice and

frozen at -80 ˚C until purification. The cells were then thawed and lysed by sonication for 3 min, three times, with a 3 min interval for each cycle. The cell lysate was centrifuged at 15,000 × g for 30 min to separate the insoluble debris. The supernatant was filtered through a 0.45 μm membrane filter and then applied to a 5 mL HisTrap FF crude column, which was pre-equilibrated with His-Binding buffer (25 mM Tris-HCl pH 7.4, 500 mM NaCl, 25 mM imidazole). The column was washed with His-Binding buffer until the absorbance of the column eluate at 280 nm stabilized, and then the Ktag-TNFα was eluted from the column using a gradient of the His-Elution buffer (25 mM Tris-HCl pH 7.4, 500 mM NaCl, 500 mM imidazole) from 0% to 100% over a volume of 25 mL. The fractions containing proteins were analyzed by SDS-PAGE to confirm the presence of the Ktag-TNFα. The fractions containing Ktag-TNFα were collected and subjected to buffer exchange into 10 mM Tris-HCl pH 7.4 using a HiPrep 26/10 Desalting column. The buffer-exchanged solution was then applied to a HiTrap SP HP column pre-equilibrated with 10 mM Tris-HCl pH 7.4. The column was washed with 25 mL of the same buffer, and then Ktag-TNFα was eluted using a gradient of the same buffer containing 500 mM NaCl from 0% to 100%. The fractions containing the target protein were collected and concentrated to about 5 mL using an ultrafiltration membrane (10 kDa MWCO). The concentrated solution was applied to a size exclusion column (HiLoad 16/600 Superdex 200 pg) that had been pre-equilibrated with 10 mM Tris-HCl (pH 8.0) and further purified by size exclusion chromatography. The fractions were analyzed with SDS-PAGE. The fractions containing Ktag-TNFα were collected and concentrated to approximately 3 mL using an ultrafiltration membrane (10 kDa MWCO) and stored at -80˚C in aliquots. Protein concentration was determined by measuring the UV absorbance at 280 nm using NanoDrop with the theoretical extinction coefficient.

4. Activity measurement of the MTG mutants

4.1 Hydroxamate assay

K10X/Y12A MTG mutants were assessed by quantifying the amount of hydroxamate resulting from MTG reaction using complex formation of hydroxamate and Fe-(III) ions[50]. Substrate solution containing 30 mM Z-QG, 100 mM hydroxylamine hydrochloride, and 10 mM glutathione in 0.2 M Tris-Acetate (pH 6.0) was added to MTG variants. After 10 min of incubation at 37 ˚C, stop solution (200 mM trichloroacetic acid in 50 mM HCl) containing 50 mM Fe-(III) chloride hexahydrate was added to the reaction mixture and the absorbance at 525 nm was measured using a Synergy HTX Multi-Mode Reader (BioTek, Winooski, USA). A standard curve was made by using L-glutamic acid γ-monohydroxamate solution of known concentrations. One unit of MTG was defined as the amount of MTG that catalyzed formation of 1 μmol of hydroxamic acid in 1 min.

4.2 GLDH-coupled assay

To determine the activity of K10R/Y12X mutants, a continuous GLDH-coupled assay of MTG activity was applied[41]. For glutamine substrate evaluation, the assay was performed in a 96-well half plate in the presence of 10 mM α-ketoglutarate, 2 U of GLDH, 500 μM NADH, 10 mM cadaverine (as amine donor substituting for a Lys peptide), 20 mM Z-Gln-Gly (as acyl-acceptor substituting for a Gln peptide), 1 mM EDTA and 200 mM MOPS buffer (pH 7.2) in a final volume of 90 μL. The reaction solution was preincubated for 10 min at 37 ˚C. Reaction was started by the addition of 1.5 μM K10R/Y12X MTGz (in a volume of 10 μL) to give a final volume of 200 μL, and the oxidation of NADH was continuously recorded at 340 nm for 60 min using a microplate reader (SpectraMax i3x, Molecular Device), controlled at 37 ˚C, with short shaking intervals before each measurement. After a short lag phase during which sufficient ammonia was produced to

483 saturate GLDH, linear slopes of absorbance versus time were measured, then the activity of MTG
484 was determined by the initial rates of NADH oxidation.
485 For the kinetic analysis of EzMTGs and an active mature MTG (ΔproMTG)[48], initial reaction
486 rates were measured by varying the concentration of Z-QG at a constant concentration of cadaver-
487 ine. Initial rate data were fitted to Michaelis-Menten kinetics, then kinetic parameters were deter-
488 mined using KaleidaGraph™ software.
489 **4.3 Thermal stability measurements**
490 Thermal stability of selected EzMTG mutants was evaluated by incubating the aqueous solution
491 of the enzyme in PBS buffer (pH 7.4) at 60 ˚C for 1 h, then the activity of MTG was determined
492 using GLDH-coupled assay.
493
494 **5. Binding affinity of mutated propeptide to the MTG active site**
495 Binding kinetics of EGFP-Propeptide mutants with ΔproMTG (without His-tag) were measured
496 using a biolayer interferometry system (BLItz) with Ni-NTA biosensors (ForteBio Inc.). Sensor
497 tips were prehydrated for 10 min in Milli-Q water and then equilibrated in K buffer (150 mM NaCl,
498 0.1% BSA, 0.002% Tween20). EGFP-propeptide mutants (100 μg/mL) were immobilized onto Ni-
499 NTA sensor tips for 2 min until the binding of protein reached saturation. A concentration series
500 of 62.5, 125, 250, 500, 1000 nM of ΔproMTG (without His-tag) was allowed for 2 min followed
501 by a 2-min dissociation step. Wild-type EGFP (100 μg/mL) and ΔproMTG (1 μM) were used as
502 negative control (data not shown). Assays were performed according to the instrument manual.
503 Data were exported from BLItz pro software and replotted. Values of binding as reflected by
504 changes in optical thickness (nm) were used to calculate each kinetic and binding constants (k_a, k_d,
505 and K_D) using nonlinear curve fitting for the entire concentration of ΔproMTG.

6. MTG-mediated labeling of K-tag TNF-α with fluorescent substrate

The reaction mixture contained TNF-α-Ktag (10 μM) and FITC-β-Ala-QG (200 μM) in PBS buffer (pH 7.4)[51]. The protein labeling reaction was initiated by the addition of MTG (0.1 μM) at 37 ˚C. To follow the time course of MTG-mediated labeling of TNF-α-Ktag with FITC-β-Ala-QG, a small aliquot of 4 × SDS-PAGE sample buffer was added to the reaction solution to terminate the MTG reaction. The reaction was followed by the increase in the fluorescence of protein bands in images of SDS-PAGE. With respect to the fluorescein derivatives, 6 μL of the reaction samples were applied to the gel. Before staining the gel with Coomassie Brilliant Blue (CBB), an image of the gel fluorescence was obtained using a Molecular Imager FX Pro (Bio-Rad Laboratories, Inc.). An excitation wavelength of 488 nm with a 530 (±15) nm band pass filter was used for the fluorescein-derivatives.

ASSOCIATED CONTENT

Supporting Information

The Supporting Information is available free of charge at doi.

Amino acid sequences of all recombinant proteins, self-labeling evaluation of MTGz mutants, scheme of enzymatic activity assays, expression of EzMTG mutants in *E. coli*, thermal treatments of selected EzMTG mutants, scheme of BLI analyses.

AUTHOR INFORMATION

Corresponding Author

Noriho Kamiya *E-mail: kamiya.noriho.367@m.kyushu-u.ac.jp.

ORCID

Ryo Sato : 0000-0002-5416-9253

Rie Wakabayashi : 0000-0003-0348-8091

Kosuke Minamihata : 0000-0002-0187-0935

Masahiro Goto : 0000-0002-2008-9351

Noriho Kamiya : 0000-0003-4898-6342

Author Contributions

R.A.: Formal Analysis, Investigation, Validation, Writing-review. **T.M.**: Formal Analysis, Investigation, Validation. **K.M.**: Formal Analysis, Methodology, Investigation, Validation, and editing. **R.S., K.H.**: Formal Analysis, Investigation. **R.W.**: Validation, and editing. **M.G.**: Resources, Validation, and editing. **N.K.**: Conceptualization, Methodology, Supervision, Validation, Writing-review, and editing.

Funding Sources

JSPS KAKENHI Grant numbers JP19H00841 and JP23H00247.

Acknowledgments

This work was supported by the Japan Society for the Promotion of Science (JSPS) KAKENHI Grant numbers JP19H00841 and JP23H00247 (to N. K.) We thank Edanz Group (https://en-author-services.edanz.com/ac) for editing a draft of this manuscript.

Abbreviations

549 MTG, microbial transglutaminase; TNF, tumor necrosis factor; EGFP, enhanced green fluorescent
550 protein; FITC, fluorescein isothiocyanate.

551

552 **References**

553 (1) Klein, T.; Eckhard, U.; Dufour, A.; Solis, N.; Overall, C. M. Proteolytic Cleavage -
554 Mechanisms, Function, and "Omic" Approaches for a Near-Ubiquitous Posttranslational
555 Modification. *Chem. Rev.* **2018**, *118* (3), 1137–1168.
556 https://doi.org/10.1021/acs.chemrev.7b00120.
557 (2) Verma, S.; Dixit, R.; Pandey, K. C. Cysteine Proteases: Modes of Activation and Future
558 Prospects as Pharmacological Targets. *Front. Pharmacol.* **2016**, *7* (APR), 1–12.
559 https://doi.org/10.3389/fphar.2016.00107.
560 (3) Dutta, S.; Choudhury, D.; Roy, S.; Dattagupta, J. K.; Biswas, S. Mutation in the Pro-
561 Peptide Region of a Cysteine Protease Leads to Altered Activity and Specificity - A
562 Structural and Biochemical Approach. *PLoS One* **2016**, *11* (6), 1–19.
563 https://doi.org/10.1371/journal.pone.0158024.
564 (4) Yokoyama, K.; Nio, N.; Kikuchi, Y. Properties and Applications of Microbial
565 Transglutaminase. *Appl. Microbiol. Biotechnol.* **2004**, *64* (4), 447–454.
566 https://doi.org/10.1007/s00253-003-1539-5.
567 (5) Di Sandro, A.; Del Duca, S.; Verderio, E.; Hargreaves, A. J.; Scarpellini, A.; Cai, G.;
568 Cresti, M.; Faleri, C.; Iorio, R. A.; Hirose, S.; Furutani, Y.; Coutts, I. G. C.; Griffin, M.;
569 Bonner, P. L. R.; Serafini-Fracassini, D. An Extracellular Transglutaminase Is Required
570 for Apple Pollen Tube Growth. *Biochem. J.* **2010**, *429* (2), 261–271.
571 https://doi.org/10.1042/BJ20100291.
572 (6) Shibata, T.; Hadano, J.; Kawasaki, D.; Dong, X.; Kawabata, S. I.; Sllner, T. Drosophila
573 TG-A Transglutaminase Is Secreted via an Unconventional Golgi-Independent Mechanism
574 Involving Exosomes and Two Types of Fatty Acylations. *J. Biol. Chem.* **2017**, *292* (25),
575 10723–10734. https://doi.org/10.1074/jbc.M117.779710.
576 (7) Griffin, D.; Casadio, R.; Bergamini, C. M. Transglutaminases: nature's biological glues.
577 *Biochem J*. **2002**, 368 (2), 377-396. https://doi.org/10.1042/bj20021234
578 (8) Lorand, L.; Graham, R. Transglutaminases: nature's biological glues. *Nat Rev Mol Cell*
579 *Biol*. **2003**, 4 (2), 140-156. https://doi.org/10.1038/nrm1014
580 (9) Strop, P. Versatility of Microbial Transglutaminase. *Bioconjug. Chem.* **2014**, *25* (5), 855–
581 862. https://doi.org/10.1021/bc500099v.
582 (10) Kashiwagi, T.; Yokoyama, K. ichi; Ishikawa, K.; Ono, K.; Ejima, D.; Matsui, H.; Suzuki,
583 E. ichiro. Crystal Structure of Microbial Transglutaminase from Streptoverticillium
584 Mobaraense. *J. Biol. Chem.* **2002**, *277* (46), 44252–44260.
585 https://doi.org/10.1074/jbc.M203933200.
586 (11) Zhang, D.; Zhu, Y.; Chen, J. Microbial Transglutaminase Production: Understanding the
587 Mechanism. *Biotechnol. Genet. Eng. Rev.* **2009**, *26* (1), 205–222.
588 https://doi.org/10.5661/bger-26-205.

(12) Ando, H.; Adachi, M.; Umeda, K.; Matsuura, A.; Nonaka, M.; Uchio, R.; Tanaka, H.; Motoki, M. Purification and Characteristics of a Novel Transglutaminase Derived from Microorganisms. *Agric. Biol. Chem.* **1989**, *53* (10), 2613–2617. https://doi.org/10.1271/bbb1961.53.2613.

(13) Takazawa, T.; Kamiya, N.; Ueda, H.; Nagamune, Enzymatic labeling of a single chain variable fragment of an antibody with alkaline phosphatase by microbial transglutaminase. *Biotechnol Bioeng*. **2004**, 86 (4), 399-404. https://doi.org/10.1002/bit.20019

(14) Abe, H.; Goto, M.; Kamiya, N. Enzymatic Single-Step Preparation of Multifunctional Proteins. *Chem. Commun.* **2010**, *46* (38), 7160–7162. https://doi.org/10.1039/c0cc02133d.

(15) Oteng-Pabi, S. K.; Pardin, C.; Stoica, M.; Keillor, J. W. Site-Specific Protein Labelling and Immobilization Mediated by Microbial Transglutaminase. *Chem. Commun.* **2014**, *50* (50), 6604–6606. https://doi.org/10.1039/c4cc00994k.

(16) Takahara, M.; Wakabayashi, R.; Fujimoto, N.; Minamihata, K.; Goto, M.; Kamiya, N. Enzymatic Cell-Surface Decoration with Proteins Using Amphiphilic Lipid-Fused Peptide Substrates. *Chem. - A Eur. J.* **2019**, *25* (30), 7315–7321. https://doi.org/10.1002/chem.201900370.

(17) Rachel, N. M.; Toulouse, J. L.; Pelletier, J. N. Transglutaminase-Catalyzed Bioconjugation Using One-Pot Metal-Free Bioorthogonal Chemistry. *Bioconjug. Chem.* **2017**, *28* (10), 2518–2523. https://doi.org/10.1021/acs.bioconjchem.7b00509.

(18) Sato, H.; Hayashi, E.; Yamada, N.; Yatagai, M.; Takahara, Y. Further Studies on the Site-Specific Protein Modification by Microbial Transglutaminase. *Bioconjug. Chem.* **2001**, *12* (5), 701–710. https://doi.org/10.1021/bc000132h.

(19) Spolaore, B.; Raboni, S.; Satwekar, A. A.; Grigoletto, A.; Mero, A.; Montagner, I. M.; Rosato, A.; Pasut, G.; Fontana, A. Site-Specific Transglutaminase-Mediated Conjugation of Interferon α-2b at Glutamine or Lysine Residues. *Bioconjug. Chem.* **2016**, *27* (11), 2695–2706. https://doi.org/10.1021/acs.bioconjchem.6b00468.

(20) Wakabayashi, R.; Yahiro, K.; Hayashi, K.; Goto, M.; Kamiya, N. Protein-Grafted Polymers Prepared Through a Site-Specific Conjugation by Microbial Transglutaminase for an Immunosorbent Assay. *Biomacromolecules* **2017**, *18* (2), 422–430. https://doi.org/10.1021/acs.biomac.6b01538.

(21) Kitaoka, M.; Tsuruda, Y.; Tanaka, Y.; Goto, M.; Mitsumori, M.; Hayashi, K.; Hiraishi, Y.; Miyawaki, K.; Noji, S.; Kamiya, N. Transglutaminase-Mediated Synthesis of a DNA-(Enzyme)n Probe for Highly Sensitive DNA Detection. *Chem. - A Eur. J.* **2011**, *17* (19), 5387–5392. https://doi.org/10.1002/chem.201003744.

(22) Strop, P.; Liu, S. H.; Dorywalska, M.; Delaria, K.; Dushin, R. G.; Tran, T. T.; Ho, W. H.; Farias, S.; Casas, M. G.; Abdiche, Y.; Zhou, D.; Chandrasekaran, R.; Samain, C.; Loo, C.; Rossi, A.; Rickert, M.; Krimm, S.; Wong, T.; Chin, S. M.; Yu, J.; Dilley, J.; Chaparro-Riggers, J.; Filzen, G. F.; O'Donnell, C. J.; Wang, F.; Myers, J. S.; Pons, J.; Shelton, D. L.; Rajpal, A. Location Matters: Site of Conjugation Modulates Stability and Pharmacokinetics of Antibody Drug Conjugates. *Chem. Biol.* **2013**, *20* (2), 161–167. https://doi.org/10.1016/j.chembiol.2013.01.010.

(23) Lhospice, F.; Brégeon, D.; Belmant, C.; Dennler, P.; Chiotellis, A.; Fischer, E.; Gauthier, L.; Boëdec, A.; Rispaud, H.; Savard-Chambard, S.; Represa, A.; Schneider, N.; Paturel, C.; Sapet, M.; Delcambre, C.; Ingoure, S.; Viaud, N.; Bonnafous, C.; Schibli, R.; Romagné, F. Site-Specific Conjugation of Monomethyl Auristatin e to Anti-CD30

Antibodies Improves Their Pharmacokinetics and Therapeutic Index in Rodent Models. *Mol. Pharm.* **2015**, *12* (6), 1863–1871. https://doi.org/10.1021/mp500666j.
(24) Dickgiesser, S.; Rieker, M.; Mueller-Pompalla, D.; Schröter, C.; Tonillo, J.; Warszawski, S.; Raab-Westphal, S.; Kühn, S.; Knehans, T.; Könning, D.; Dotterweich, J.; Betz, U. A. K.; Anderl, J.; Hecht, S.; Rasche, N. Site-Specific Conjugation of Native Antibodies Using Engineered Microbial Transglutaminases. *Bioconjug. Chem.* **2020**, *31* (4), 1070–1076. https://doi.org/10.1021/acs.bioconjchem.0c00061.
(25) Yurimoto, H.; Yamane, M.; Kikuchi, Y.; Matsui, H.; Kato, N.; Sakai, Y. The Pro-Peptide of Streptomyces Mobaraensis Transglutaminase Functions in Cis and in Trans to Mediate Efficient Secretion of Active Enzyme from Methylotrophic Yeasts. *Biosci. Biotechnol. Biochem.* **2004**, *68* (10), 2058–2069. https://doi.org/10.1271/bbb.68.2058.
(26) Liu, S.; Zhang, D.; Wang, M.; Cui, W.; Chen, K.; Du, G.; Chen, J.; Zhou, Z. The Order of Expression Is a Key Factor in the Production of Active Transglutaminase in Escherichia Coli by Co-Expression with Its pro-Peptide. *Microb. Cell Fact.* **2011**, *10*, 1–7. https://doi.org/10.1186/1475-2859-10-112.
(27) Chen, Y. J.; Inouye, M. The Intramolecular Chaperone-Mediated Protein Folding. *Curr. Opin. Struct. Biol.* **2008**, *18* (6), 765–770. https://doi.org/10.1016/j.sbi.2008.10.005.
(28) Bryan, P. N. Prodomains and Protein Folding Catalysis. *Chem. Rev.* **2002**, *102* (12), 4805–4815. https://doi.org/10.1021/cr010190b.
(29) Zotzel, J.; Keller, P.; Fuchsbauer, H. L. Transglutaminase from Streptomyces Mobaraensis Is Activated by an Endogenous Metalloprotease. *Eur. J. Biochem.* **2003**, *270* (15), 3214–3222. https://doi.org/10.1046/j.1432-1033.2003.03703.x.
(30) Zotzel, J.; Pasternack, R.; Pelzer, C.; Ziegert, D.; Mainusch, M.; Fuchsbauer, H. L. Activated Transglutaminase from Streptomyces Mobaraensis Is Processed by a Tripeptidyl Aminopeptidase in the Final Step. *Eur. J. Biochem.* **2003**, *270* (20), 4149–4155. https://doi.org/10.1046/j.1432-1033.2003.03809.x.
(31) Marx, C. K.; Hertel, T. C.; Pietzsch, M. Soluble Expression of a Pro-Transglutaminase from Streptomyces Mobaraensis in Escherichia Coli. *Enzyme Microb. Technol.* **2007**, *40* (6), 1543–1550. https://doi.org/10.1016/j.enzmictec.2006.10.036.
(32) Rickert, M.; Strop, P.; Lui, V.; Melton-Witt, J.; Farias, S. E.; Foletti, D.; Shelton, D.; Pons, J.; Rajpal, A. Production of Soluble and Active Microbial Transglutaminase in Escherichia Coli for Site-Specific Antibody Drug Conjugation. *Protein Sci.* **2016**, *25*, 442–455. https://doi.org/10.1002/pro.2833.
(33) Takehana, S.; Takagi, H.; Motoki, M.; Washizu, K.; Ando, K.; Koikeda, S.; Takeuchi, K. Chemical Synthesis of the Gene for Microbial Transglutaminase from Streptoverticillium and Its Expression in Escherichia Coli. *Biosci. Biotechnol. Biochem.* **1994**, *58* (1), 88–92. https://doi.org/10.1271/bbb.58.88.
(34) Sugimura, Y.; Hosono, M.; Wada, F.; Yoshimura, T.; Maki, M.; Hitomi, K. Screening for the Preferred Substrate Sequence of Transglutaminase Using a Phage-Displayed Peptide Library: Identification of Peptide Substrates for TGase 2 and Factor XIIIa. *J. Biol. Chem.* **2006**, *281* (26), 17699–17706. https://doi.org/10.1074/jbc.M513538200.
(35) Rachel, N. M.; Quaglia, D.; Lévesque, É.; Charette, A. B.; Pelletier, J. N. Engineered, Highly Reactive Substrates of Microbial Transglutaminase Enable Protein Labeling within Various Secondary Structure Elements. *Protein Sci.* **2017**, *26* (11), 2268–2279. https://doi.org/10.1002/pro.3286.

(36) Milczek, E. M. Commercial Applications for Enzyme-Mediated Protein Conjugation: New Developments in Enzymatic Processes to Deliver Functionalized Proteins on the Commercial Scale. *Chem. Rev.* **2018**, *118* (1), 119–141. https://doi.org/10.1021/acs.chemrev.6b00832.
(37) Deweid, L.; Neureiter, L.; Englert, S.; Schneider, H.; Deweid, J.; Yanakieva, D.; Sturm, J.; Bitsch, S.; Christmann, A.; Avrutina, O.; Fuchsbauer, H. L.; Kolmar, H. Directed Evolution of a Bond-Forming Enzyme: Ultrahigh-Throughput Screening of Microbial Transglutaminase Using Yeast Surface Display. *Chem. - A Eur. J.* **2018**, *24* (57), 15195–15200. https://doi.org/10.1002/chem.201803485.
(38) Tsukiji, S.; Nagamune, T. Sortase-mediated ligation: a gift from Gram-positive bacteria to protein engineering. *Chembiochem*. **2009**, 10 (5), 787-798. https://doi.org/10.1002/cbic.200800724
(39) Steffen, W.; Ko, F. C.; Patel, J.; Lyamichev, V.; Albert, T. J.; Benz, J.; Rudolph, M. G.; Bergmann, F.; Streidl, T.; Kratzsch, P.; Boenitz-Dulat, M.; Oelschlaegel, T.; Schraeml, M. Discovery of a Microbial Transglutaminase Enabling Highly Site-Specific Labeling of Proteins. *J. Biol. Chem.* **2017**, *292* (38), 15622–15635. https://doi.org/10.1074/jbc.M117.797811.
(40) Yang, M. Te; Chang, C. H.; Wang, J. M.; Wu, T. K.; Wang, Y. K.; Chang, C. Y.; Li, T. H. T. Crystal Structure and Inhibition Studies of Transglutaminase from Streptomyces Mobaraense. *J. Biol. Chem.* **2011**, *286* (9), 7301–7307. https://doi.org/10.1074/jbc.M110.203315.
(41) Oteng-Pabi, S. K.; Keillor, J. W. Continuous Enzyme-Coupled Assay for Microbial Transglutaminase Activity. *Anal. Biochem.* **2013**, *441* (2), 169–173. https://doi.org/10.1016/j.ab.2013.07.014.
(42) Marx, C. K.; Hertel, T. C.; Pietzsch, M. Random Mutagenesis of a Recombinant Microbial Transglutaminase for the Generation of Thermostable and Heat-Sensitive Variants. *J. Biotechnol.* **2008**, *136* (3–4), 156–162. https://doi.org/10.1016/j.jbiotec.2008.06.005.
(43) Ohtake, K.; Mukai, T.; Iraha, F.; Takahashi, M.; Haruna, K. I.; Date, M.; Yokoyama, K.; Sakamoto, K. Engineering an Automaturing Transglutaminase with Enhanced Thermostability by Genetic Code Expansion with Two Codon Reassignments. *ACS Synth. Biol.* **2018**, *7* (9), 2170–2176. https://doi.org/10.1021/acssynbio.8b00157.
(44) Abdiche, Y.; Malashock, D.; Pinkerton, A.; Pons, J. Determining Kinetics and Affinities of Protein Interactions Using a Parallel Real-Time Label-Free Biosensor, the Octet. *Anal. Biochem.* **2008**, *377* (2), 209–217. https://doi.org/10.1016/j.ab.2008.03.035.
(45) Do, T.; Ho, F.; Heidecker, B.; Witte, K.; Chang, L.; Lerner, L. A Rapid Method for Determining Dynamic Binding Capacity of Resins for the Purification of Proteins. *Protein Expr. Purif.* **2008**, *60* (2), 147–150. https://doi.org/10.1016/j.pep.2008.04.009.
(46) Pinkas, D. M.; Strop, P.; Brunger, A. T.; Khosla, C. Transglutaminase 2 Undergoes a Large Conformational Change upon Activation. *PLoS Biol.* **2007**, *5* (12), 2788–2796. https://doi.org/10.1371/journal.pbio.0050327.
(47) Klöock, C.; Khosla, C. Regulation of the Activities of the Mammalian Transglutaminase Family of Enzymes. *Protein Sci.* **2012**, *21* (12), 1781–1791. https://doi.org/10.1002/pro.2162.
(48) Liu, S.; Cerione, R. A.; Clardy, J. Structural Basis for the Guanine Nucleotide-Binding Activity of Tissue Transglutaminase and Its Regulation of Transamidation Activity. *Proc.*

Natl. Acad. Sci. U. S. A. **2002**, *99* (5), 2743–2747. https://doi.org/10.1073/pnas.042454899.

(49) Sato, R.; Minamihata, K.; Ariyoshi, R.; Taniguchi, H.; Kamiya, N. Recombinant Production of Active Microbial Transglutaminase in E. Coli by Using Self-Cleavable Zymogen with Mutated Propeptide. *Protein Expr. Purif.* **2020**, *176* (July), 105730. https://doi.org/10.1016/j.pep.2020.105730.

(50) FOLK, J. E.; COLE, P. W. Structural Requirements of Specific Substrates for Guinea Pig Liver. *J. Biol. Chem.* **1965**, *240* (7), 2951–2960.

(51) Kamiya, N.; Abe, H.; Goto, M.; Tsuji, Y.; Jikuya, H. Fluorescent Substrates for Covalent Protein Labeling Catalyzed by Microbial Transglutaminase. *Org. Biomol. Chem.* **2009**, *7* (17), 3407–3412. https://doi.org/10.1039/b904046c.

TOC graphic

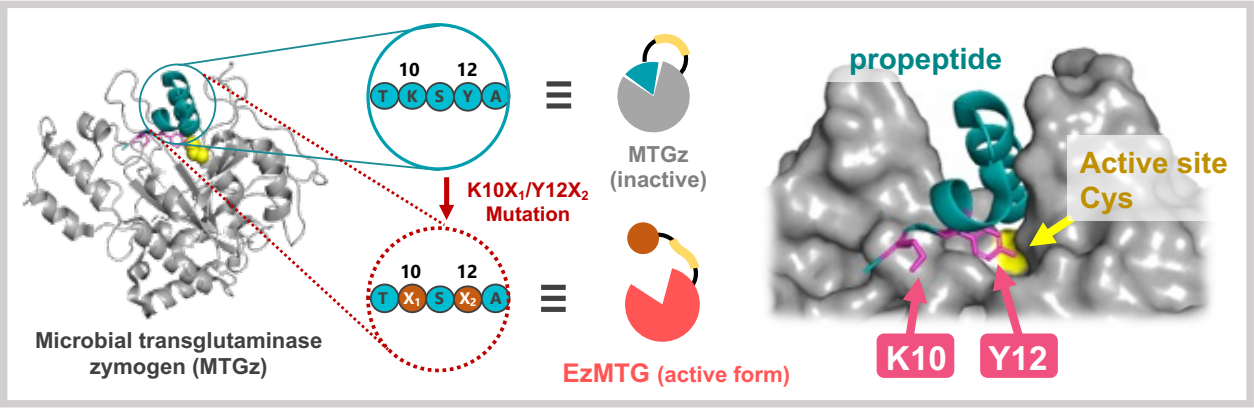

Double point mutations in the propeptide region of microbial transglutaminase generated active microbial transglutaminase zymogen exhibiting unique substrate specificities toward peptidyl substrates.